Progress In Electromagnetics Research M, Vol. 54, 75–82, 2017

The Two-Slit Interference of Vector Optical Fields with Both Radially and Azimuthally Variant States of Polarization

Tengyue Gao, Chaoyang Qian, Xiaoyu Zhang, and Rui-Pin Chen*

Abstract—The interference behaviors of a vector optical field with both radially and azimuthally variant states of polarization (SoP) through the Young's two-slits are theoretically studied. The optical field distribution with periodic stripes in the far field results from the interference of the vector optical field through the Young's two-slits with different initial SoP distributions. It is found that the far-field distribution can be manipulated by the incident vector optical field with the initial phase and SoP distributions. Particularly, the distribution of radially-variant SoP in the cross-section of the incident optical field provides an additional freedom to control the interference patterns of the x-component, y-component and total intensity distribution in far field. This approach provides a new method to further expand the functionality of an optical system by considering the distribution of SoP in field cross-section.

1. INTRODUCTION

Recently, the studies about the vector optical field have attracted great interest due to its novel properties and potential applications [1–4]. Compared to a scalar optical field with the uniform distribution of states of polarization (SoP), the vector optical field with nonuniform distribution of SoP in the field cross-section has many unique properties and potential applications on corresponding fields such as optical devices, optical trapping and micro-particle manipulation [5–7]. The current studies about the vector optical field are mainly focused on the manipulation of an optical field, characteristics of the focusing and propagation of a vector optical field, and their corresponding applications [8–12]. In particular, the generation of a vector optical field, focusing characteristics of a vector optical field and its propagation dynamics were demonstrated theoretically and experimentally [13–17]. The nonlinear dynamics of a vector optical field with different SoP distributions have been demonstrated [18, 19]. The evanescent wave part and near-field characteristics of a vector optical field have been studied [20]. As a fundamental experiment in an optics context, the double-slit experiment was performed originally by Thomas Young in 1801 and played a vital part in the acceptance of the wave theory of light. Generally, the Young's double-slit interference experiment is performed with a scalar beam (i.e., with a uniform polarization in the cross-section of an optical field) [21]. More recently, the interference behaviors of a vector optical field with azimuthally variant SoP through the young's double-slits were explored [22]. The interference patterns in far field were analyzed in relation with the topological charge and initial phase of a vector optical field. However, a vector optical field can combine both radially and azimuthally variant SoP distributions. In particular, the radially variant SoP distributions will also contribute to interference patterns of the different components in far field. Therefore, the distribution of radially-variant SoP provides an additional freedom to control the interference pattern in far field including intensity, phase and polarization. The modern double-slit experiment is a demonstration that light and matter can display characteristics of both classically defined waves and particles; moreover, it displays

Received 17 November 2016, Accepted 7 January 2017, Scheduled 9 February 2017
* Corresponding author: Rui-Pin Chen (chenrp@zstu.edu.cn).
The authors are with the Department of Physics, Zhejiang Sci.-Tech. University, Hangzhou 310018, China.

the fundamentally probabilistic nature of quantum mechanical phenomena [23]. Obviously, exploring the interference behavior of a vector optical field with hybrid SoP can benefit deeper understanding of the nature of light [23, 24]. The vectorial effect of an optical field with hybrid SoP in the field cross-section leads to different interference behaviors [25] and may find potential applications in corresponding field.

In this work, we study the novel interference behaviors of a vector optical field with both radially and azimuthally variant SoP distributions through the two-slits. Compared to the double-slit interference of a scalar optical field [26] and a vector optical field with azimuthally variant polarization, the double-slit interference phenomena with both radially and azimuthally variant polarizations provide a deeper understanding about the characteristics of the vector field and their interference characteristics. With different distributions of the initial SoP, the interference fringes in far field appear in different shapes. In particular, with the modulation of radially variant polarization, the interference patterns in far field have more complex interference fringes of the x and y components. These results provide a new method to further expand the functionality of an optical system and thus can find potential applications in the manipulation of an optical field [1–3], nonlinear optics [18, 19], imaging [6], and quantum optics [7, 23, 24].

2. THEORETICAL FORMULATION

In the polar coordinate system, the z-axis is taken to be the direction of light propagation. A cylindrical optical vector field with both radially and azimuthally variant SoP distributions can be expressed as [15, 16]

$$E(r,\theta) = A_0\ [\cos(m\theta + 2\pi l(r/r_0) + \theta_0)\vec{e}_x + \sin(m\theta + 2\pi l(r/r_0) + \theta_0)\vec{e}_y], \tag{1}$$

where $r = (x^2 + y^2)^{1/2}$ and $\theta = \arctan(y/x)$ are the polar radius and azimuthal angle in the polar coordinate system, respectively. m is the topological charge, and θ_0 is the initial phase. e_x and e_y are the unit vectors in x- and y-directions, respectively. l is an integer associated with the radially variant SoP distribution. A_0 is the amplitude and thereafter setting $A_0 = 1$ for simplicity. The schematic diagram and demonstration of the two-slit interference are shown in Fig. 1.

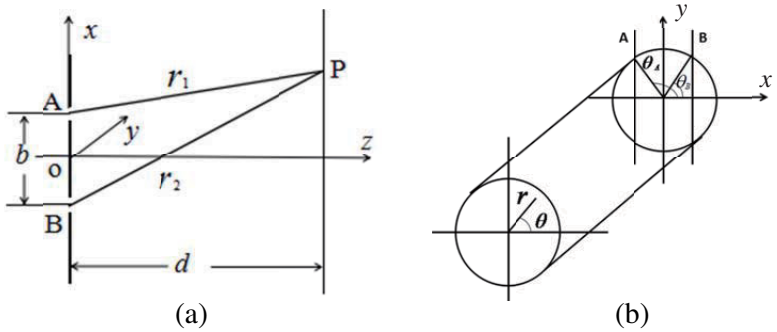

Figure 1. (Color online). (a) Double-slit device schematic diagram; (b) Vector beam cross section before and after passage through the double slit.

There are two slits A and B in the x-y plane, and the distance between the two slits is b. Slits A and B are perpendicular to x axis, and the width of the two slits is a. The distance between the observation plane which is parallel to the x-y plane and the plane where the two slits are located is d. According to Eq. (1), the vector optical field can be decomposed into x and y direction components:

$$E_x(r,\theta) = \cos[m\theta + 2\pi l(r/r_0) + \theta_0], \tag{2}$$

$$E_y(r,\theta) = \sin[m\theta + 2\pi l(r/r_0) + \theta_0]. \tag{3}$$

When light beam is incident on the two slits, A and B, the x and y components interfer independently. According to the double-beam interference intensity formula [27]:

$$I = E_A^2 + E_B^2 + 2E_A E_B \cos\delta, \tag{4}$$

where E_A and E_B are the optical fields at the two slits positions, respectively. $\delta = 2\pi bx/(\lambda d)$ is the phase difference between E_A and E_B. As recognized from Fig. 1, any two relative points at two slits are symmetrical about y axis. Their azimuthal angles θ_A and θ_B are supplementary, namely $\theta_A = \pi - \theta_B$, and their polar radius $r_A = r_B = b/(2\cos\theta_B)$. The x components of E_A and E_B can be written as: $E_A = \cos\varphi_A$, $E_B = \cos\varphi_B$ where $\varphi_A = m\theta_A + 2\pi l(r_A/r_0) + \theta_0$, $\varphi_B = m\theta_B + 2\pi l(r_B/r_0) + \theta_0$. On the other hand, y components of E_A and E_B are: $E_A = \sin\varphi_A$, $E_B = \sin\varphi_B$. According to Eq. (4), the interference intensity distributions of x and y components in the observation plane therefore can be expressed as:

$$I_x(x,y) = \cos^2\varphi_A + \cos^2\varphi_B + 2\cos\varphi_A\cos\varphi_B\cos\delta, \tag{5}$$

$$I_y(x,y) = \sin^2\varphi_A + \sin^2\varphi_B + 2\sin\varphi_A\sin\varphi_B\cos\delta. \tag{6}$$

And the total light intensity distribution is:

$$I(x,y) = I_x(x,y) + I_y(x,y) = 2 - 2\cos(2m\theta_B)\cos\delta. \tag{7}$$

3. NUMERICAL RESULTS AND ANALYSIS

In order to further explore the interference patterns of the vector optical field with radially and azimuthally variant polarization distributions through the double slits, the numerical calculations are

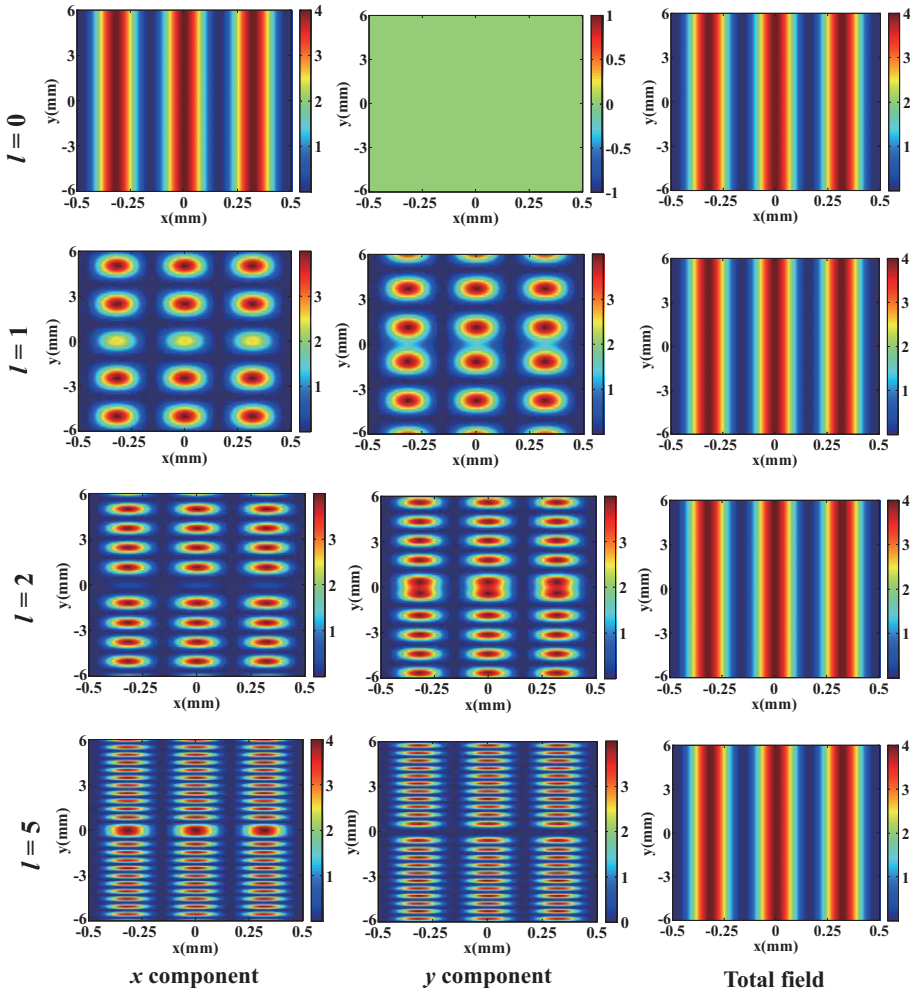

Figure 2. (Color online). Patterns of the Young's two-slit interference of the vector optical fields after passage through the double slit for $m = 0$ with $\theta_0 = 0$ and $l = 0$, 1, 2, 5.

performed according to Eqs. (5)–(7) with $\lambda = 632.6\,\text{nm}$, $r_0 = 5\,\text{mm}$, $d = 500\,\text{mm}$ and $b = 1\,\text{mm}$. The corresponding results of x, y components and the total intensity distributions are shown in Figs. 2–6 for different parameters m, θ_0 and l. The novel properties of the interference patterns are found with different initial SoPs, especially in the center parts of the interference patterns. Different from the well-known Young's two-slit interference of the scalar light field, the interference patterns of the vector optical fields exhibit the spatial structure in the y (slit) direction besides in the x direction as shown in Figs. 2–6. The interference patterns of the x component and y component are sensitively relative to parameters l, m and θ_0. However, the interference pattern of the total field depends only on parameter m but independent of parameters l and θ_0. In particular, the interference fringes in the central parts in the observation plane are modulated by both x and y components. Note that when $m = 0$, $l = 0$ and $\theta_0 = 0$, the interference patterns are for a conventional scalar optical field as shown in the first row of Fig. 2.

Figures 2–4 show the different interference patterns of the vector optical fields for $m = 0$, 1 and 2 with $\theta_0 = 0$ and $l = 0$, 1, 2 and 5, respectively. If $m = 0$ and $l = 0$, the light intensity distribution of x-component and the total field in far-field are the same, and the intensity of y-component is zero as shown in Fig. 2. This is because the incident optical field with $m = 0$, $\theta_0 = 0$ and $l = 0$ degenerate the uniform distribution of the polarization (i.e., a scalar optical field). When $l \neq 0$, the optical field possesses a radially variant polarization distribution in the field cross section, the bright stripes and dark stripes appear alternately in the central parts of the interference patterns of x and y components. Away from the center of the interference patterns, the intensity distributions of x and y components is becoming more and more similar. With increasing values of l, the stripes are becoming more narrow. However, the total field distributions are always the same despite the variant values of l. These phenomena can be recognized from Eqs. (5)–(7) that the values of φ_A and φ_B in the middle region of the optical field will change more quickly with the increasing values of l which leads to the intensity distributions of x component and y component in the central region changing more quickly.

The interference patterns for the vector fields $m = 1$, 2, 5 with $l = 0$ and $\theta_0 = 0$ are shown in

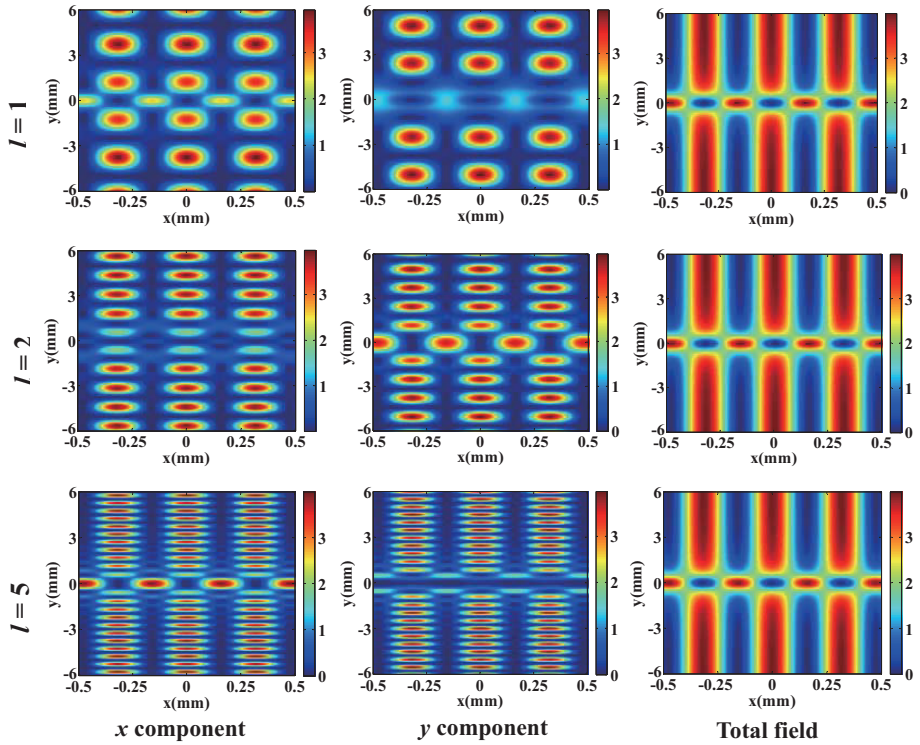

Figure 3. (Color online). Patterns of the Young's two-slit interference of the vector optical fields after passage through the double slit for $m = 1$ with $\theta_0 = 0$ and $l = 1$, 2, 5.

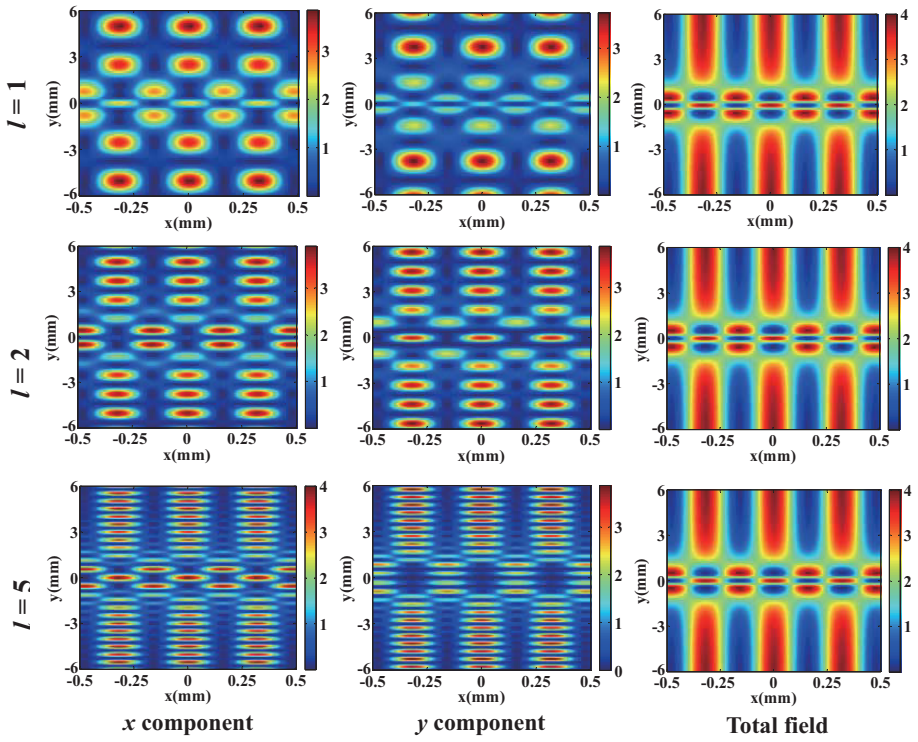

Figure 4. (Color online). Patterns of the Young's two-slit interference of the vector optical fields after passage through the double slit for $m = 2$ with $\theta_0 = 0$ and $l = 1$, 2, 5.

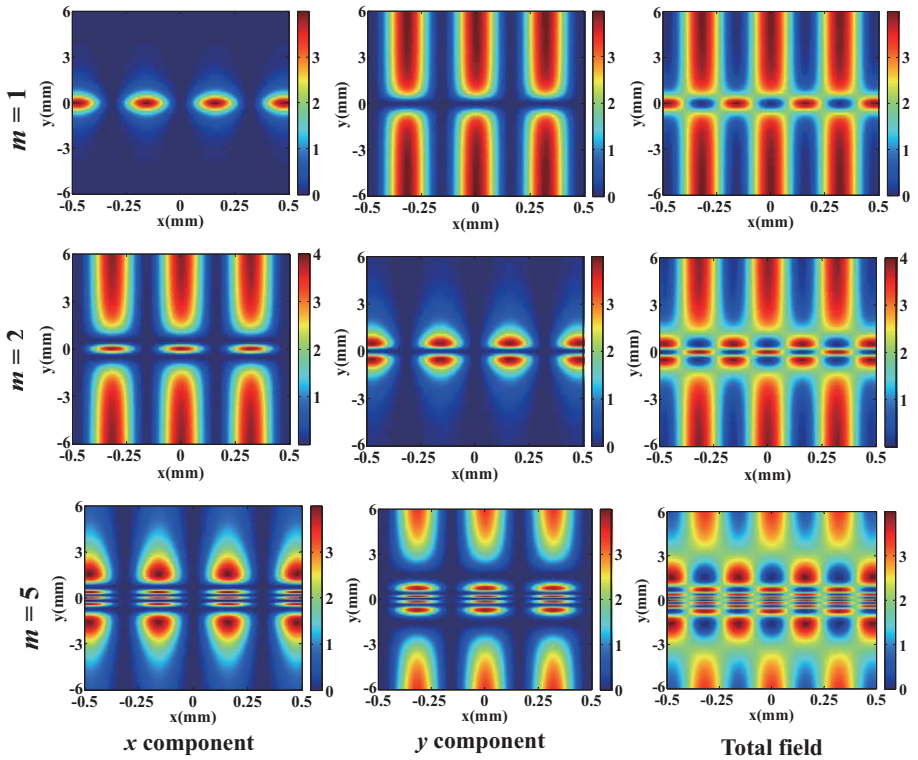

Figure 5. (Color online). Patterns of the Young's two-slit interference of the vector optical fields after passage through the double slit with $l = 0$, $\theta_0 = 0$ and $m = 1$, 2, 5.

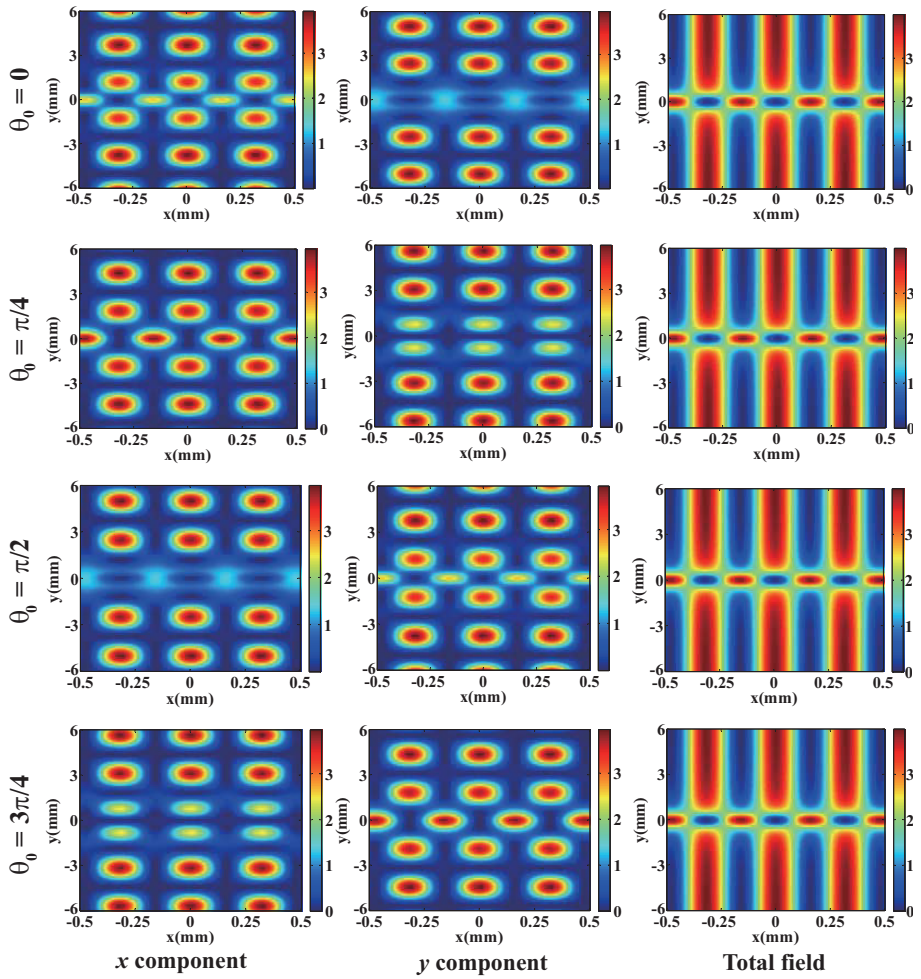

Figure 6. (Color online). Patterns of the Young's two-slit interference of the vector optical fields after passage through the double slit with $l = 1$, $m = 1$ and $\theta_0 = 0$, $\pi/4$, $\pi/2$, $3\pi/4$.

Fig. 5. It can be found that the interference fringes of x component, y component and the total field exhibit a chessboard structure in the middle region, and the number of squares in the checkerboard will increase with the increasing values of m. The total number of bright and dark regions is $2m - 1$. In this case for $l = 0$ and $\theta_0 = 0$, the vector field is degenerated as an optical field with azimuthally variant SoP distribution in the field cross-section, but no variant in radial direction. The interference pattern is the same as the experimental results as shown in [22]. Fig. 6 shows interference patterns for the vector fields $\theta_0 = 0$, $\pi/4$, $\pi/2$, $3\pi/4$ with $l = 1$ and $m = 1$. One can find that the intensity distributions of y component with $\theta_0 = 0$ and x component with $\theta_0 = \pi/2$ are the same. In a similar way, the intensity distributions of y component with $\theta_0 = \pi/4$ and x component with $\theta_0 = 3\pi/4$ are the same. This phenomenon can be explained by the initial vector optical field as described in Eqs. (1)–(3). As recognized from Eqs. (1)–(3), the x components of initial vector optical field with $\theta_0 = \pi/2$ and $\theta_0 = 3\pi/4$ are equal to that of the y components of initial vector optical field with $\theta_0 = 0$ and $\theta_0 = \pi/4$.

4. CONCLUSION

The interference behaviors of the vector fields with both radially and azimuthally variant polarizations in two slits have been demonstrated. The results reveal that the interference pattern of the total intensity is determined by the topological charge of the initial vector field m. However, the interference patterns of x and y components are related to the initial phase θ_0 and radially variant polarization parameter l

of the initial vector field. In particular, with the modulation of radially variant SoP in the cross-section of the incident optical field, the interference patterns in far field indicate complex interference fringes of x and y components. The interference patterns of x-component, y-component and the total intensity distributions can be manipulated by the initial distributions of SoP in the field cross-section. These results provide a new method to further expand the functionality of an optical system and thus can find potential applications in the corresponding fields.

ACKNOWLEDGMENT

This work is partially supported by the National Natural Science Foundation of China under Grant No. 11574271, the Zhejiang Provincial Natural Science Foundation under Grant No. LQ13A040001 the Science Research Foundation of Zhejiang Sci-Tech University (ZSTU) under Grant No. 14062078-Y.

REFERENCES

1. Litchinitser, N. M., "Structured light meets structured matter," *Science*, Vol. 337, 1054–1055, 2012.
2. Chen, R. P., Z. Chen, K. H. Chew, P. G. Li, Z. Yu, J. Ding, and S. He, "Structured caustic vector vortex optical field: Manipulating optical angular momentum flux and polarization rotation," *Scientific Reports*, Vol. 5, 10628, 2015.
3. Waller, E. H. and G. Freymann, "Independent spatial intensity, phase and polarization distribution," *Optics Express*, Vol. 21, 28167–28174, 2013.
4. Chen, R. P., K. H. Chew, B. Gu, and G. Zhou, "Effect of a spiral phase on a vector beam with hybrid polarization states," *Journal of Optics*, Vol. 17, 065605, 2015.
5. Bomzon, Z., V. Kleiner, and E. Hasman, "Computer-generated space-variant polarization elements with subwavelength metal stripes," *Optics Letters*, Vol. 26, 33–35, 2001.
6. Chen, R., K. Agarwal, J. R. Colin, Sheppard, and X. D. Chen, "Imaging using cylindrical vector beams in a high numerical-aperture microscopy system," *Optics Letters*, Vol. 38, 3111–3114, 2013.
7. Visser, J., E. R. Elier, and G. Nierhuis, "Polarization entanglement in a crystal with three fold symmetry," *Physical Review A*, Vol. 66, 033814, 2002.
8. Dorn, R., S. Quabis, and G. Leuchs, "Sharper focus for a radially polarized beam," *Physical Review Letters*, Vol. 91, 233901, 2003.
9. Tian, B. and J. Pu, "Tight focusing of a double-ring-shaped azimuthally polarized beam," *Optics Letters*, Vol. 36, 2014–2016, 2011.
10. Gu, B., Y. Pan, L. J. Wu, and Y. P. Cui, "Tight focusing properties of spatial-variant linearly-polarized vector beams," *Journal of Optics*, Vol. 43, 18–27, 2013.
11. Hu, K. L., Z. Y. Chen, and J. X. Pu, "Tight focusing properties of hybridly polarized vector beams," *Journal of Optical Society of America A*, Vol. 29, 1099–1101, 2012.
12. Deng, D., Q. Guo, L. Wu, and X. Yang, "Propagation of radially polarized elegant light beams," *Journal of Optical Society of America B*, Vol. 24, 636–643, 2007.
13. Wang, X. L., J. P. Ding, W. J. Ni, C. S. Guo, and H. T. Wang, "Generation of arbitrary vector beams with a spatial light modulator and a common path interferometric arrangement," *Optics Letters*, Vol. 32, 3549–3551, 2007.
14. Wang, X. L., Y. N. Li, J. Chen, C. S. Guo, J. P. Ding, and H. T. Wang, "A new type of vector fields with hybrid states of polarization," *Optics Express*, Vol. 18, 10786–10795, 2010.
15. Chen, H., J. J. Hao, B. F. Zhang, J. Xu, J. P. Ding, and H. T. Wang, "Generation of vector beam with space-variant distribution of both polarization and phase," *Optics Letters*, Vol. 36, 3179–3181, 2011.
16. Han, W., Y. F. Yang, W. Cheng, and Q. W. Zhan, "Vectorial optical field generator for the creation of arbitrarily complex fields," *Optics Express*, Vol. 21, 20692–20793, 2013.
17. Lerman, G. M., L. Stern, and U. Levy, "Generation and tight focusing of hybridly polarized vector beams," *Optics Express*, Vol. 18, 27650–27657, 2010.

18. Li, S. M., Y. Li, X. L. Wang, L. J. Kong, K. Lou, C. Tu, Y. Tian, and H. T. Wang, "Taming the collapse of optical fields," *Scientific Reports*, Vol. 2, 1007, 2012.
19. Chen, R. P., L. X. Zhong, K. H. Chew, T. Y. Zhao, and X. Zhang, "Collapse dynamics of a vector vortex optical field with inhomogeneous states of polarization," *Laser Physics*, Vol. 25, 075401, 2015.
20. Chen, R. P. and G. Li, "The evanescent wavefield part of a cylindrical vector beam," *Optics Express*, Vol. 21, 22246–22254, 2013.
21. Setala, T., J. Tervo, and A. T. Frberg, "Stokes parameters and polarization contrasts in Young's interference experiment," *Optics Letters*, Vol. 31, 208–210, 2006.
22. Li, Y. N., X. L. Wang, H. Zhao, L. J. Kong, K. Lou, B. Gu, C. G. Tu, and H. T. Wang, "Young's two-slit interference of vector light fields," *Optics Letters*, Vol. 37, 1790–1792, 2012.
23. Wootters, W. W. and W. H. Zurek, "Complementarity in the double-slit experiment: Quantum nonseparability and quantitative statement of Bohr's principle," *Phys. Rev. D*, Vol. 19, 473–484, 1979.
24. Svensson, B. E. Y., "Pedagogical review of quantum measurement theory with an emphasis on weak measurements," *Quanta*, Vol. 2, 18–49, 2013.
25. Cai, F., J. Yu, and S. He, "Vectorial electric field Monte Caro simulations for focused laser beams (800 nm–2220 nm) in a biological sample," *Progress In Electromagnetics Research*, Vol. 142, 667–681, 2013.
26. Imran, A. and Q. A. Naqvi, "Diffraction of plane wave by two parallel slits in an infinitely long impedance plane using the method of Kobayashi potential," *Progress In Electromagnetics Research*, Vol. 63, 107–123, 2006.
27. Born, M. and E. Wolf, *Principles of Optics*, 7th Edition, Cambridge U. Press, 1999.